

Synchronization Analysis for Wireless TWRC Operated with Physical-layer Network Coding

Shengli Zhang · Soung-Chang Liew · Hui Wang

© Springer Science+Business Media, LLC. 2011

Abstract Physical-layer network coding (PNC) makes use of the additive nature of the electromagnetic waves to apply network coding arithmetic at the physical layer. With PNC, the destructive effect of interference in wireless networks is eliminated and the capacity of networks can be boosted significantly. This paper addresses a key outstanding issue in PNC: synchronization among transmitting nodes. We first investigate the impact of imperfect synchronization in a 3-node network with a straightforward detection scheme. It is shown that with QPSK modulation, PNC on average still yields significantly higher capacity than straightforward network coding when there are synchronization errors. Significantly, this remains to be so even in the extreme case when synchronization is not performed at all. Moving beyond a 3-node network, we propose and investigate a synchronization scheme for PNC in a general chain network. And we argue that if the synchronization errors can be bounded in the 3-node case, they can also be bounded in the general N -node case. Lastly, we present simulation results showing that PNC is robust to synchronization errors. In particular, for the mutual information performance, there is about 2 dB loss without phase or symbol synchronization.

Keywords Physical-layer network coding · Wireless networks · Synchronization

S. Zhang (✉) · H. Wang
Department of Communication Engineering, Shenzhen University,
Shenzhen, China
e-mail: zsl@szu.edu.cn

H. Wang
e-mail: wanghsz@szu.edu.cn

S.-C. Liew
Department of Information Engineering, The Chinese University of Hong Kong,
Hong Kong, People's Republic of China
e-mail: soung@ie.cuhk.edu.hk

1 Introduction

One of the biggest challenges in wireless communication is how to deal with the interference at the receiver when signals from multiple sources arrive simultaneously. In the radio channel of the physical layer of wireless networks, data are transmitted through electromagnetic (EM) waves in a broadcast manner (electromagnetic (EM) waves transmitted by any node can be heard by all the nodes nearby). The interference from these EM waves causes the data to be scrambled. While interference has a negative effect on wireless networks in general, its detrimental effect on the throughput/capacity for both cellular networks and *multi-hop* ad hoc networks is particularly noticeable [1–3].

Most communication system designs try to either reduce or avoid interference (e.g., through receiver design or transmission scheduling [1]). However, instead of treating interference as a nuisance to be avoided, we can actually embrace interference to improve throughput performance. To do so in a multi-hop network, we previously proposed physical-layer network coding (PNC) in [4] to create an apparatus similar to that of network coding, but which performs network coding arithmetic at the lower physical layer using the additive property of EM signal reception. Through a proper modulation-and-demodulation technique at relay nodes, addition of EM signals can be mapped to $GF(2^n)$ addition of digital bit streams, so that the interference effect becomes part of the arithmetic operation in network coding. For more information on PNC, please refer to [29, 30].

Two levels of synchronization between the two end-nodes were assumed in PNC in [4], namely symbol-level time synchronization, and carrier- frequency/phase synchronization. In this paper, we first investigate the impact of imperfect synchronization (i.e., finite synchronization errors) on PNC in a 3-node network with QPSK modulation. It is shown that PNC still yields significantly higher capacity than straightforward network coding under imperfect synchronization. Significantly, this remains so even in the extreme case when synchronization is not performed at all. Moving beyond the 3-node linear network, we propose a synchronization scheme for PNC in the N -node linear network. The N -node network can be decomposed into a chain of 3-node PNC units for synchronization purposes. If channel coding is applied on each of the 3-node PNC units, then the performance in terms of the end-to-end capacity will be the same for the N -node network and the 3-node network.

1.1 Related Work

Synchronization has long been an active research problem in wireless networks. Here, we review prior work on synchronization relevant to the 3-node PNC case. First, symbol time and carrier-frequency synchronizations, which are needed in PNC, have been actively investigated by researchers in many fields such as OFDMA, wireless-sensor network, and cooperative transmission. In particular, methods for joint estimation of carrier-frequency error, symbol timing error and channel response have been proposed for OFDMA networks [5, 6], and methods for symbol synchronization have been proposed in wireless sensor networks [7, 8]. All these methods can be borrowed to realize the symbol time and frequency synchronization in PNC. PNC needs accurate carrier phase synchronization (which also implies very accurate carrier frequency synchronization) between the transmitters, which has recently been studied in the field of coherent cooperation (distributed beam forming) to synchronize the separately distributed nodes. Among all these schemes, the most direct scheme uses beacons, which are transmitted between the destination (relay) node and the source (end) nodes, to estimate the relative phase offsets, so that each source can adjust its phase to compensate for this offset before transmitting [9]. To reduce the high feedback bandwidth required in [9], a one

bit feedback synchronization scheme is proposed in [10]. Experiments in [10] showed that the scheme has good performance. Some open loop algorithms without the iterative information exchange between the destination and the source nodes have also been proposed. For example, positive results have been obtained in [11] with a master-slave architecture to prove the feasibility of the distributed beam forming technique. In [12, 13], another open loop synchronization scheme, round trip synchronization, were proposed and discussed where a beacon is used to measure round trip phase delays among the transmitters and the destination. We can apply the ideas in these schemes to synchronize the phase of the two end nodes in our three-node PNC scheme. Besides the proposed synchronization algorithms, people also analyzed the effect of the synchronization errors in the coherent cooperate transmissions. For example, a more realistic collaborative communication system that includes the influence of AWGN and phase error on the signal transmission was analyzed in [14]. However, the analysis in [14] is different from the analysis in our paper here, since the source nodes in [14] transmit the same signal while the source nodes in our paper transmit different signals.

We previously studied the synchronization effects of PNC with BPSK modulation in [22]. In this paper, we substantially extended those results to the case of QPSK modulation. The phase offset has little effect for BPSK modulation while it can affect the performance significantly in the QPSK case.

The rest of this paper is organized as follows. Section 2 presents the system model and illustrates the basic idea of PNC with a linear 3-node network under the assumption of perfect synchronization. Section 3 analyzes the performance penalty of non-perfect synchronization on PNC. Section 4 proposes a strategy to extend 3-node synchronization method to an N -node PNC chain. Section 5 studies the performance penalty of non-perfect synchronization by numerical simulation, and Sect. 6 concludes the paper.

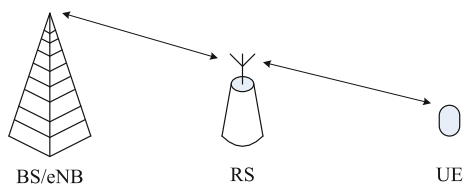
2 System Model and Illustrating Example

2.1 System Model

In this paper, we focus on two-way relay channels (TWRC). A typical TWRC is the three-node relay channel as shown in Fig. 1. The *BS* (base station) and *UE* (User Equipment) are nodes that exchange information, but they are out of each other's transmission range. The *RS* (relay station) is the relay node between them. In LTE-advanced, the relay related standard released allows wireless *RS* to be deployed to relay information between the *BS* and the *UE*. This system model may also find application in satellite communication, where the satellite serves as a relay to facilitate information exchange between two mobile stations on the earth.

We consider frame-based communication in which a time slot is defined as the time required for the transmission of one fixed-size frame. In this paper, a frame is denoted by a capital letter and a symbol within the frame is denoted by the corresponding small letter. Each node is equipped with an omni-directional antenna, and the channel is half duplex so

Fig. 1 Two way transmission between base station (BS) and UE (user equipment) through the relay station (RS)



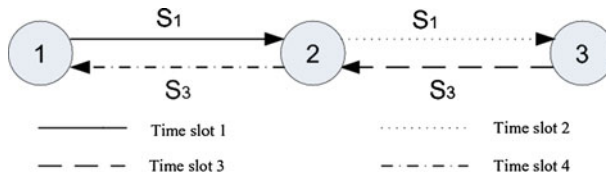


Fig. 2 Traditional scheduling scheme

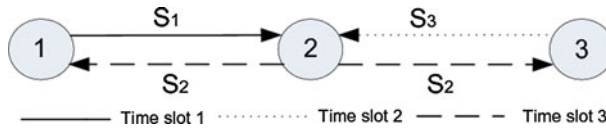


Fig. 3 Straightforward network coding scheme

that transmission and reception at a particular node must occur in different time slots. We assume that QPSK modulation is employed at all the nodes.

2.2 Physical-Layer Network Coding Scheme

Before introducing the PNC transmission scheme, we first describe the traditional transmission scheduling scheme and the “straightforward” network-coding scheme for mutual exchange of a frame in the 3-node network [15, 16].

The traditional transmission schedule is given in Fig. 2. Let S_i denote the frame initiated by N_i . N_1 first sends S_1 to N_2 , and then N_2 relays S_1 to N_3 . After that, N_3 sends S_3 in the reverse direction. A total of four time slots are needed for the exchange of two frames in opposite directions.

References [15] and [16] outline the straightforward way of applying network coding in the 3-node wireless network. Figure 3 illustrates the idea. First, N_1 sends S_1 to N_2 and then N_3 sends frame S_3 to N_2 . After receiving S_1 and S_3 , N_2 encodes them to obtain the frame $S_2 = S_1 \oplus S_3$, where \oplus denotes bitwise exclusive OR operation being applied over the entire frames of S_1 and S_3 . N_2 then broadcasts S_2 to both N_1 and N_3 . When N_1 (N_3) receives S_2 , it extracts S_3 (S_1) from S_2 using the local information S_1 (S_3). A total of three time slots are needed, for a throughput improvement of 33% over the traditional transmission scheduling scheme.

We now introduce PNC. For the time being, let us also assume perfect symbol-level time, carrier synchronization (we will remove this assumption in later sections), and the use of power control, so that the frames from N_1 and N_3 arrive at N_2 with the same phase and amplitude. The combined passband signal received by N_2 during one symbol period is

$$\begin{aligned}
 r_2(t) &= s_1(t) + s_3(t) \\
 &= [a_1 \cos(\omega t) + b_1 \sin(\omega t)] + [a_3 \cos(\omega t) + b_3 \sin(\omega t)] \\
 &= (a_1 + a_3) \cos(\omega t) + (b_1 + b_3) \sin(\omega t)
 \end{aligned} \tag{1}$$

where $S_i(t)$, $i = 1$ or 3 , is the passband signal transmitted by N_i and $r_2(t)$ is the passband signal received by N_2 during one symbol period, a_i and b_i are the QPSK modulated information bits (in-phase and quadrature-phase respectively) of N_i ; and ω is the carrier frequency. Then, N_2 will receive two baseband signals, in-phase (I) and quadrature phase (Q), respectively, as follows:

Table 1 PNC mapping: modulation mapping at N_1, N_3 ; demodulation and modulation mappings at N_2

Modulation mapping at N_1 and N_3				Demodulation mapping at N_2		
Input		Output		Input	Output	
				Modulation mapping at N_2		
				Input	Output	
$S_1^{(I)}$	$S_3^{(I)}$	a_1	a_3	$a_1 + a_3$	$S_2^{(I)}$	a_2
1	1	1	1	2	0	-1
0	1	-1	1	0	1	1
1	0	1	-1	0	1	1
0	0	-1	-1	-2	0	-1

$$\begin{aligned}
 r^I &= a_1 + a_3 \\
 r^Q &= b_1 + b_3.
 \end{aligned}
 \tag{2}$$

Note that N_2 cannot extract the individual information transmitted by N_1 and N_3 , i.e., a_1, b_1, a_3 and b_3 , from its received combined signal r^I and r^Q . However, N_2 is just a relay node and it does not care what the information is. As long as N_2 can transmit the necessary information to N_1 and N_3 for extraction of a_1, b_1, a_3, b_3 over there, the end-to-end delivery of information will be successful. For this, all we need is a special modulation/demodulation mapping scheme, referred to as *PNC mapping*, to obtain the equivalence of GF(2) summation of bits from N_1 and N_3 at the physical layer.

Table 1 illustrates the idea of PNC mapping. In Table 1, $S_j^{(I)} \in \{0, 1\}$ is a variable representing the in-phase data bit of N_j and $a_j \in \{-1, 1\}$ is a variable representing the binary modulated bit of $S_j^{(I)}$ such that $a_j = 2s_j^{(I)} - 1$. A similar table (not shown here) can also be constructed for the quadrature-phase data by letting $S_j^{(Q)} \in \{0, 1\}$ be the quadrature data bit of N_j , and $b_j \in \{-1, 1\}$ be the binary modulated bit of $S_j^{(Q)}$ such that $b_j = 2s_j^{(Q)} - 1$.

With reference to Table 1, N_2 obtains the data bits:

$$s_2^{(I)} = s_1^{(I)} \oplus s_3^{(I)}; \quad s_2^{(Q)} = s_1^{(Q)} \oplus s_3^{(Q)}.
 \tag{3}$$

The successively derived $S_2^{(I)}$ and $S_2^{(Q)}$ bits within a time slot will then be used to form the frame S_2 . In other words, the operation $S_2 = S_1 \oplus S_3$ in straightforward network coding can now be realized through PNC mapping. The relay then transmits, according to the QPSK modulation mapping,

$$s_2(t) = a_2 \cos(\omega t) + b_2 \sin(\omega t).
 \tag{4}$$

Upon receiving $S_2(t)$, N_1 and N_3 can derive $S_2^{(I)}$ and $S_2^{(Q)}$ by ordinary QPSK demodulation.

As illustrated in Fig. 4, PNC requires only two time slots for the exchange of one frame (as opposed to three time slots in straightforward network coding).

In [4], we analyzed the bit error rate (BER) of $S_1 \oplus S_3$ at the relay node for PNC scheme and the straightforward network coding scheme. It was shown that PNC slightly outperforms the straightforward network coding scheme, and slightly underperforms the standard point-to-point BPSK transmission. When the per-hop BER is low, the end-to-end BER for the three schemes is very similar. The main advantage of PNC, however, is the reduced number of

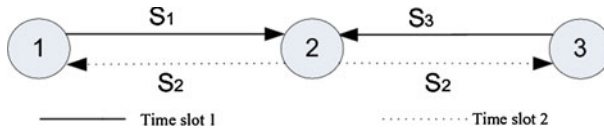


Fig. 4 Physical layer network coding

time slots needed. In this paper, we showed that this conclusion is true even without perfect synchronization.

3 Performance Penalty of Synchronization Errors

The basic PNC scheme presented thus far requires symbol-time, carrier-frequency and carrier-phase synchronizations, although these requirements could be relaxed for other variations of PNC [17, 18, 25–28]. We now consider the performance penalty of synchronization errors on PNC¹ with a straightforward detection scheme. This framework is applicable to situations where synchronization is not perfect (e.g., synchronization may become imperfect with time due the changing characteristics of the channel) as well as when synchronization is not performed at all. The discussion here is based on the 3-node model in Sect. 2.

3.1 Penalty of Carrier-Frequency/Phase Synchronization Errors

We first consider carrier-phase and carrier-frequency errors. For QPSK modulation, the two received signals from node N_1 and N_3 can be written as:

$$r_2(t) = [a_1 \cos(\omega t) + b_1 \sin(\omega t)] + [a_3 \cos((\omega + \Delta\omega)t + \Delta\theta) + b_3 \sin((\omega + \Delta\omega)t + \Delta\theta)] \quad (5)$$

where $\Delta\theta$ is the phase offset and $\Delta\omega$ is the frequency offset. Here we assume that the relative carrier-phase offset of the two input signals is known to the receiver.² The receiver down-converts the passband signal to the baseband to obtain a symbol in the packet

$$\begin{aligned} r_2 &= s_1 + s_3 \\ &= [a_1 + b_1] + [a_3 \cos(\Delta\omega T + \Delta\theta) - a_3 \sin(\Delta\omega T + \Delta\theta) + b_3 \cos(\Delta\omega T \\ &\quad + \Delta\theta) + b_3 \sin(\Delta\omega T + \Delta\theta)] \\ &= [a_1 + b_1] + \sqrt{2}[a_3 \cos(\theta) + b_3 \cos(\theta)] \end{aligned} \quad (6)$$

where T is the symbol duration and $\theta = \Delta\omega T + \Delta\theta + \pi/4$ is the final phase offset generated by the carrier frequency offset and the carrier phase offset. Hereafter, we only consider the

¹ Our paper tries to show the advantages of PNC over traditional and straightforward schemes even with synchronization errors. Although the power synchronization error (amplitude offset between the two end-node signals¹) also affects the PNC performance, the result is mainly determined by the signal with smaller power [24, 27], which is similar to the traditional and straightforward schemes [23]. Therefore, we do not analyze the power synchronization error penalty in this paper. We also assume line of sight transmission in this paper and the effects of multipath is a future work.

² Before the adjacent transmitters transmit their data concurrently as per PNC, they could first take turns transmitting a preamble in a non-overlapping manner. The receiver can then derive the phase difference from the two preambles. Frequency and time offsets can be similarly determined using preambles. Note that this is different from synchronization, since the transmitters do not adjust their phase, frequency and symbol-time differences thereafter. The receiver simply accepts the synchronization errors the way they are.

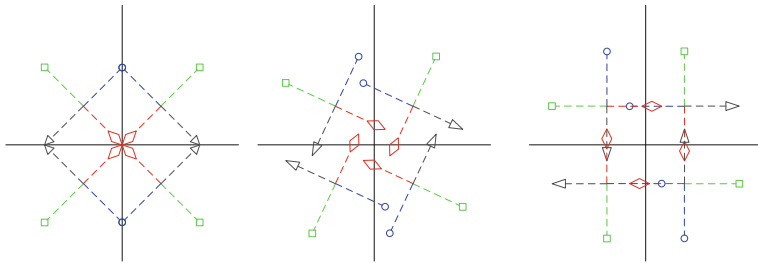


Fig. 5 Constellations of superimposed baseband signals in (6) with phase difference θ equal to 0° , 15° , and 45° . There are four possible values for S_1 (i.e., $S_1 = \pm 1 \pm j$) as indicated by the four line intersections in the second subfigure. In each subfigure, we show the four possible values for r_2 given each of the S_1 . The resulting constellation points with the same shape correspond to the same value of $S_1 \oplus S_3$

final phase offset θ without differentiating the contributions of carrier phase from carrier frequency offset. Note that we only need to deal with the case when $-\pi/4 \leq \theta < \pi/4$. If $\theta = \theta' + k \cdot \frac{\pi}{2}$ and $-\pi/4 < \theta' \leq \pi/4$, we can simply replace a_3 with $a'_3 = a_3 \cdot e^{k\pi/2}$, and replace θ with $\theta' = \theta - k\pi/2$; a'_3 can be mapped back to a_3 in a unique manner after detection at the end nodes.

In Fig. 5, we plot the received signal with different phase differences. From this figure, we can see that as the phase difference θ increases from 0 to $\pi/4$ (or decreases from 0 to $-\pi/4$), a constellation point of $s_1 \oplus s_3$ may break into several points and the distance between the points of different $s_1 \oplus s_3$ may increase or decrease. The BER performance of demodulating $s_1 \oplus s_3$ from the received signal in Fig. 5 is dominated by the minimum distance between constellation points of different $s_1 \oplus s_3$. As shown in Fig. 5, given the phase difference $0 \leq \theta \leq \pi/4$, the minimum square distance, denoted by d , between the points of different $s_1 \oplus s_3$ is

$$d^2 = 4(1 - \cos \theta)^2 + 4(1 - \sin \theta)^2 \tag{7}$$

We now bound the equivalent power penalty caused by the phase difference θ by benchmark against a reference system. The transmit power of each source in the original system is 2. Consider a reference system in which the transmit power of each source is $P \leq 2$. With perfect phase synchronization, the minimum distance between adjacent points of different $s_1 \oplus s_3$ of the reference system is $2\sqrt{P/2}$. We can tune P such that the minimum distance of the reference system is shortened to the minimum distance of the PNC system with phase difference θ , i.e., $2\sqrt{P/2} = d$. Effectively, the power penalty of the system with phase difference θ is $P/2$ (note that P is the effective power and 2 is the actual power in the system with phase difference, θ). In particular, the BER performance of the PNC system with nonzero θ is better than that of the reference system with zero θ and with power thus adjusted. This is because decreasing the transmit power in the reference system reduces the distances among all the different constellation points uniformly, while in the original system, the phase difference reduces the distances between some constellation points and enlarges other distances. In other words, the performance loss of the phase difference θ is upper bounded by a power penalty given as follows:

$$\Delta\gamma(\theta) \leq P/2 = d^2/4 = (1 - \cos \theta)^2 + (1 - \sin |\theta|)^2 - \frac{\pi}{4} \leq \theta \leq \frac{\pi}{4}. \tag{8}$$

In Fig. 6, we plot the upper bound in (8) with different phase offset. We can see that the power penalty bound is more than 7 dB when the phase offset is about $\pm\pi/4$. However, we need not be too pessimistic. When there is no synchronization, a reasonable assumption is that

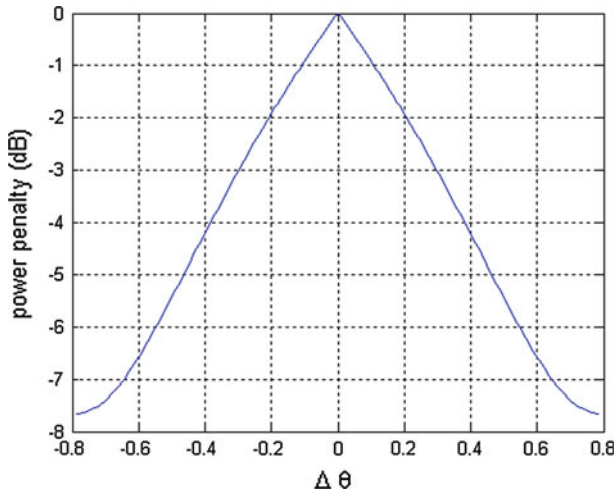


Fig. 6 Power penalty upper bound of carrier phase and frequency synchronization errors

the phase offset is uniformly distributed over $[-\pi/4, \pi/4]$. In this case, the average upper bounded power penalty is

$$\begin{aligned} \overline{\Delta\gamma(\theta)} &= \frac{2}{\pi} \int_{-\pi/4}^{\pi/4} \Delta\gamma(\theta) d\theta \leq \frac{4}{\pi} \int_0^{\pi/4} (1 - \cos \theta)^2 + (1 - \sin \theta)^2 d\theta \quad (9) \\ &= -3.4 \text{ dB} \end{aligned}$$

That is, even if carrier phase synchronization is not performed at all, the average SNR penalty is upper bounded by 3.4 dB (the simulation in Fig. 12 shows that the average power penalty is only about 1.5 dB at a typical SNR of 6 dB). To avoid the worst-case penalty and to obtain the average power penalty performance, the transmitters could intentionally change their phases from symbol to symbol using a “phase increment” sequence known to the receivers (or intentionally increase their carrier frequency). If the phase-increment sequences of the two transmitters are not correlated, then certain symbols are received with low error rates and certain symbols are received with high error rates during a data packet transmission. With good forward error control (FEC) coding, the overall packet error rate can be reduced. This essentially translates the power penalty to data-rate penalty.

For a general wireless network, the SNR loss of PNC can be compensated by the smaller interference. For 1-D case, the SIR of PNC in [19, eq. (6)] is about 15.3 dB, and it is about 11.9 dB after subtracting the 3.4 dB SIR loss. While the SIR of the traditional 1-D transmission scheme is

$$\begin{aligned} \text{SIR} &= \frac{P_0/d^\alpha}{\sum_{l=0}^{\infty} P_0 \{2/[(2+4l)d]^\alpha + 1/[(3+4l)d]^\alpha + 1/[(5+4l)d]^\alpha\}} \quad (10) \\ &= 8.5 \text{ dB} \end{aligned}$$

where P_0 is the transmission power, d is the distance between adjacent nodes, and the fading coefficient α is set to a typical value of 4. For the 2-D case, the SIR of PNC is 13.5 dB with $J = 5$ is the distance between adjacent PNC chains as in [19, Eq. (9)], and it is 10.1 dB after subtracting the 3.4 dB loss. It still satisfies the target 10dB SIR requirement as used in

traditional wireless networks [19]. Therefore, even after taking into account the 3.4 dB loss upper bound due to phase asynchrony, PNC may still have a better throughput in the 1-D network and 2-D network than conventional schemes [19].

3.2 Penalty of Time Synchronization Errors

Reference [20] analyzes the impact of time synchronization errors on the performance of cooperative MISO systems, and show that the clock jitters as large as 10% of the bit period actually do not have much negative impact on the BER performance of the system. Based on the similar methodology, we can also analyze the impact of time synchronization error toward the performance of PNC.

In this section, we assume perfect carrier phase and frequency synchronizations for simplicity. In this case, the performance of QPSK is the same as that of BPSK, and therefore we only consider the in-phase signals hence. Let Δt be the symbol offset between the two input signals. The two transmitted in-phase signals can be written as:

$$\begin{aligned} s_1(t) &= \sum_{l=-\infty}^{\infty} a_1[l] \cos(2\pi ft) g(t - lT) \\ s_3(t) &= \sum_{l=-\infty}^{\infty} a_3[l] \cos(2\pi ft) g(t - lT - \Delta t) \end{aligned} \quad (11)$$

where, $a_j[l]$ is the l th bit of the real part of signal $S_j(t)$, and $g(t)$ is the pulse shaping signal. The received signal can then be written as

$$\begin{aligned} r_2(t) &= r_1(t) + r_3(t) \\ &= \sum_l a_1[l] g(t - lT) + a_3[l] g(t - lT - \Delta t). \end{aligned} \quad (12)$$

The simple receiving scheme is as follows. After the matched filter, the receiver samples the signal at time instances $t = kT + \Delta t/2$ (i.e., at the middle of the offset).³ We then have the baseband expression as

$$\begin{aligned} r_2[k] &= r_1[k] + r_3[k] \\ &= \sum_l \{a_1[l] p((k-l)T + \Delta t/2) + a_3[l] p((k-l)T - \Delta t/2)\} \\ &= (a_1[k] + a_3[k]) p(\Delta t/2) \\ &\quad + \sum_{l, l \neq k} \{a_1[l] p((k-l)T + \Delta t/2) + a_3[l] p((k-l)T - \Delta t/2)\} \end{aligned} \quad (13)$$

where, $p(t)$ is the output of the receiving filter, which matches to the input pulse $g(t)$. As widely used in practice, the raised cosine pulse shaping function, $p(t) = \frac{\sin(\pi t/T) \cos(\pi \beta t/T)}{\pi t/T \cdot (1 - 4\beta^2 t^2/T^2)}$, is chosen in our paper. We see that the time synchronization errors not only decrease the desired signal power, but also introduce inter-symbol interference (ISI). Therefore, we use SINR (signal over noise and interference ratio) penalty here to evaluate the performance degradation. The SINR penalty can be calculated as

³ When the symbol time offset is known to the relay node, the receiver may have other choices such as discarding the inter-symbol interfering part and only take the non-interfering part into account to further improve the performance.

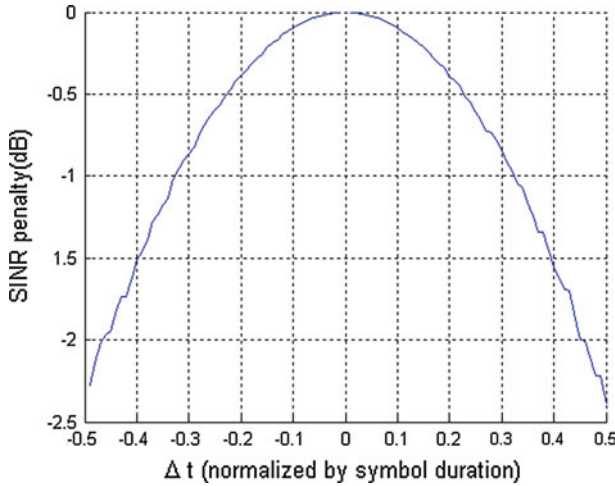


Fig. 7 Power penalty of time synchronization errors

$$\begin{aligned} \Delta\gamma(\Delta t) &= \text{SINR}(\Delta t) - \text{SNR}_0 \\ &= 10 \log_{10}(p(\Delta t/2))^2 - 10 \log_{10}\left(\frac{\sigma_{\text{ISI}}^2 + \sigma_n^2}{\sigma_n^2}\right) \end{aligned} \tag{14}$$

where $\sigma_{\text{ISI}}^2 = E\{(\sum_{l,l \neq k} a_1[l]p((k-l)T + \Delta t/2) + a_2[l]p((k-l)T - \Delta t/2))^2\}$ is the variance of the inter-symbol interference and σ_n^2 is the variance of Gaussian noise. Figure 7 plots the power penalty versus $\Delta t/T$, where the SNR_0 , i.e., $1/\sigma_n^2$, is set to 10 dB and the roll factor of the raised cosine function is set to 0.5. The worst-case SIR penalty, which is occurred when $\Delta t = T/2$, is about -2.2 dB. If we assume the time synchronization error to be uniformly distributed over $[-T/2, T/2]^4$, we can calculate the average SIR penalty as

$$\overline{\Delta\gamma} = \int_{-0.5}^{0.5} \Delta\gamma(\tau) d\tau = \int_{-0.5}^{0.5} \text{SINR}(\tau) d\tau - \text{SNR}_0 = -1.57 \text{ dB}. \tag{15}$$

When uncoded BER or mutual information is concerned, the simulation results in Sect. 5 show that the performance penalty due to non-perfect time synchronization ($-0.2T$ - $0.2T$) is less than 1 dB, which is even smaller than the SINR penalty in (15). Compared to the penalty caused by phase synchronization error in (9), our PNC scheme is more sensitive to the phase offset than the symbol time offset. This fact reminds us that we could adjust the integration time of the match filter at the relay node from T to T' ($T' \leq T$). Then, the phase offset at the relay is changed from $\theta = \Delta\omega T + \Delta\theta + \pi/4$ to a new value $\theta = \Delta\omega T' + \Delta\theta + \pi/4$. As a result, we may obtain a smaller phase offset (according to the value of $\Delta\omega$, $\Delta\theta$) at the cost of more time synchronization errors.

Based on the discussion in this section, we can conclude that the performance degradation of 3 to 4 dB due to various synchronization errors (including large carrier phase, frequency, and time synchronization errors in the case where a synchronization mechanism is not used

⁴ This assumption is reasonable since one end node can intentionally increase each symbol duration by T/N (N is the number of symbols in one packet) while the other end node keeps its own symbol duration T . As a result, all possible symbol misalignments are experienced at the relay node.

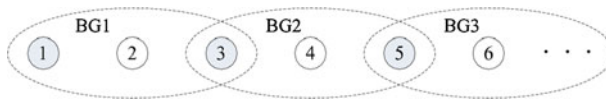


Fig. 8 Synchronization for multiple nodes



Fig. 9 Partitioning of time into synchronization phase and data-transmission phase

at all) is encountered and it is acceptable given the smaller interference of PNC ([19, Eqs. (6) and (9)]) and given the more than 100% throughput improvement obtained by PNC.

4 Synchronization in N-node PNC Chain

In the previous section, we argue that PNC detection is not very sensitive to synchronization errors in the case of $N = 3$. It may appear at first glance that the synchronization problem of the N -node case may cause PNC to break down for large N , due to the propagation of synchronization errors along the chain. Here, we argue that the detection scheme in PNC does not break down just because N is large. In particular, we argue that if the synchronization errors can be bounded in the 3-node case, they can also be bounded in the general N -node case as follows.

Synchronization between multiple sources and one destination has been extensively studied in previous works [5–14]. We assume that the feasibility of synchronization in a 3-node chain is a given based on these prior results (i.e., the two end nodes are the sources and the relay is the destination in the set-up of the 3-node chain). Let us consider how the N -node case can make use of 3-node synchronization. A possible approach is to partition the long chain into multiple 3-node local groups, as illustrated in Fig. 8, and then synchronize them in a successive manner. Suppose that the synchronization for 3-node can be achieved with reasonable error bounds for phase, frequency, and time (see Sect. 3, where we argue that PNC detection is not very sensitive to synchronization errors), represented by, say, $\theta, 2\Delta\omega, \Delta t$. An issue is the impact of these errors on the N -node chain.

For N -node synchronization, let us divide the time into two parts: the synchronization phase and the data-transmission phase, as shown in Fig. 9. These two phases are repeated periodically, say once every T_P seconds. The synchronization phase lasts T_S seconds and the data transmission phase lasts T_D seconds, with $T_S + T_D = T_P$. The PNC data transmission described in Sect. 2 comes into play only during the data transmission phase. The synchronization overhead is T_S/T_P , with T_S depending on the synchronization handshake overhead, and T_P depending on the speed at which the synchronizations drift as time progresses. That is, the faster the drift, the smaller the T_P , because one will then need to perform resynchronization more often. It turns out that the N -node case increases the T_S required, but not the $1/T_P$ required as compared to the 3-node case, as detailed below.

For the N -node chain, let us further divide the synchronization phase into two sub-phases. The first sub-phase is responsible for synchronizing all the odd-numbered⁵ nodes and the

⁵ Numbering the nodes may be accomplished during the routing phase by inserting a field in the routing protocol.

second for all the even-numbered nodes. We describe only sub-phase 1 here (sub-phase 2 is similar). With reference to Fig. 8, we divide the N nodes into $M = \lfloor (N - 1)/2 \rfloor$ basic groups (BGs) and denote them by BG j , where j is index of the BGs. Let Δt_{BG} be the time needed to synchronizing the two odd nodes in one BG (using, say, one of the prior methods proposed by others). Consider BG1. Let us assume that it is always the case that the right node (in this case, node 3) attempts to synchronize to the left node (in this case, node 1). As an example of the synchronization scheme, node 2 may estimate the frequency difference and phase difference of the signals from node 1 and node 3. Node 2 then forwards the differences to node 3 for it to adjust its own frequency and phase. After this synchronization, the phase, frequency and time errors between nodes 1 and 3 become very small and are denoted by θ , $2\Delta f$, Δt respectively. In the next Δt_{BG} time, we then synchronize node 5 to node 3 in BG2. So, a total time of $M\Delta t_{\text{BG}}$ are needed in sub-phase 1. Including sub-phase 2, $T_S = (N - 2)\Delta t_{\text{BG}}$.

It turns out that with a cleverer scheme, sub-phase 2 can be eliminated and T_S can be reduced roughly by half. But that is not the main point we are trying to make here. The main issue is that with the above method, the bounds of the synchronization errors of node N with respect to node 1 become $M\theta$, $2M\Delta\omega$, $M\Delta t$ at most and these errors grow in an uncontained manner as N increases! In particular, will PNC therefore break down as N increases?

Recall that for PNC detection, a receiver receives signals simultaneously from only the two adjacent nodes. By applying a channel coding scheme [21] at all the nodes, the relay node can recover $S_1 \oplus S_2$ from the received signal without any error. Only the synchronization error penalty within one BG can affect the PNC performance and the penalty will not propagate to other BGs. For example, say, N is odd. The reception at node 2 depends only on the synchronization between nodes 1 and 3; and the reception at node $N - 1$ only depends on the synchronization of nodes $N - 2$ and N . In particular, it is immaterial that there is a large synchronization error between nodes 1 and N . So, the fact that the end-to-end synchronization errors have grown to $M\theta$, $2M\Delta\omega$, $M\Delta t$ is not important. Only the local synchronization errors, θ , $2\Delta\omega$, Δt , are important. The same reasoning also leads us to conclude that how often synchronization should be performed (i.e., $1/T_P$) does not increase with N either, since it is only the drift within 3 nodes that are important as far as PNC detection is concerned.

Of course, T_S (overhead T_S/T_P) grows with N , but only linearly. If $N\Delta t_{\text{BG}}$ is small compared with T_P , this is not a major concern. In practice, however, we may still want to impose a limit on the chain size N not just to limit the overhead T_S , but also for other practical considerations, such as routing complexities, network management, etc. On the other hand, a larger N means a larger transport capacity [31], which is widely used to measure the network capacity. In this sense, the transport capacity, $(N - 1)T_D/(T_D + (N - 2)\Delta t_{\text{BG}})$, increases rather than decreases as N increases. Therefore, PNC may be preferable with large N .

5 Numerical Simulation

In this section, we evaluate the performance loss due to non-perfect synchronization in PNC by numerical simulation. In our simulation, QPSK modulation is used. SNR is defined as the transmission power of each end node over the variance of the Gaussian noise, i.e., $1/\sigma_n^2$ and the channel coefficient is set to 1 for simplicity.

We first show the equivalent SNR with different synchronization levels in Fig. 10. Without phase synchronization (random phase), there is about 1.5 dB loss at a given SNR of 10 dB. This SNR loss is much smaller than the upper bound of 3.4 dB in (9). The average SNR loss without time synchronization (random time offset) is very close to the result in (15). With an imperfect synchronization, the SNR loss becomes much smaller.

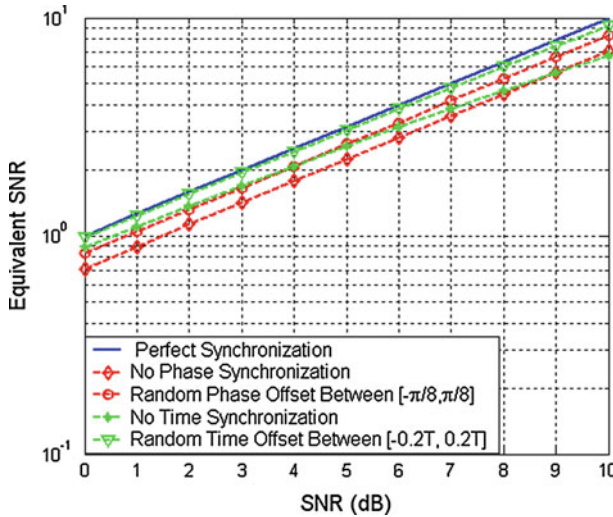


Fig. 10 Equivalent SNR of PNC with different synchronization errors

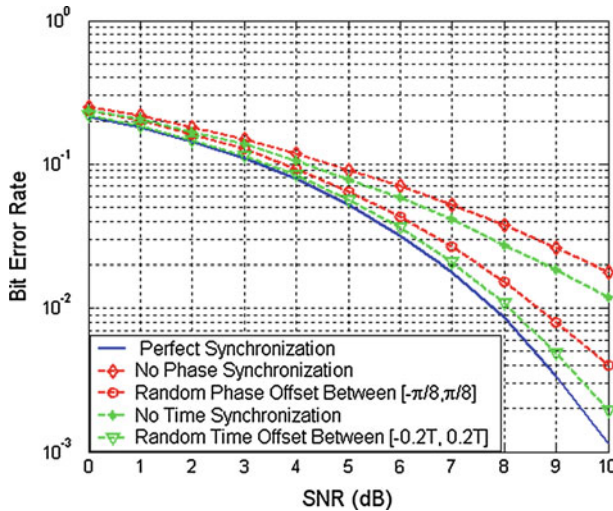


Fig. 11 uncoded BER performance of PNC with different synchronization levels

We then compare the BER performance with different synchronization levels as in Fig. 11. In this figure, the un-coded BER of $s_1 \oplus s_2$ at the relay node is plotted under different SNRs. The decision rule under perfect synchronization is the same as that in [4], the decision rule for non-perfect phase synchronization is based on ML detection⁶ and the decision rule for non-perfect symbol-time synchronization is also the same as that in [4].⁷ From this figure, we

⁶ The complexity of ML detection is high and may be impractical for large constellation size in coded system. In this paper, we focus on the performance loss due to asynchronization and ML detection corresponds to the minimum performance loss with given asynchronization.

⁷ This decision rule for non-perfect time synchronization is not optimal and it can be further improved. In that light, the obtained performance in Fig. 11 is only a lower bound.

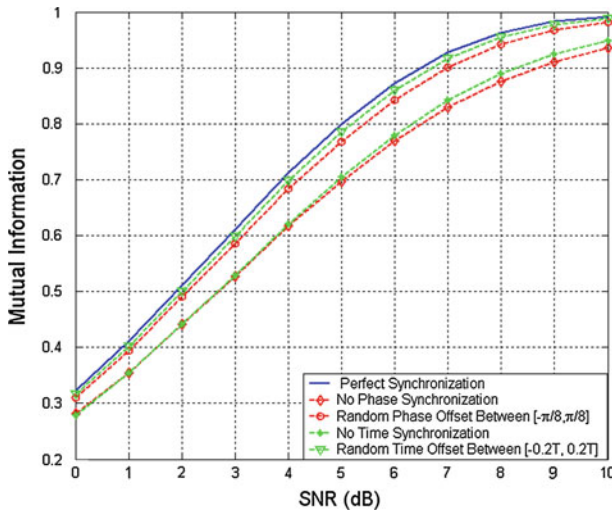


Fig. 12 Mutual information performance of PNC with different synchronization levels

can see that there is about 2.5 dB loss when no symbol-time synchronization is performed, and the performance loss decreases to 0.4 dB when the symbol time offset is randomly distributed in $[-0.2T, 0.2T]$. When there are phase synchronization errors, an SNR loss of about 3 dB can be observed at a BER of $1E-2$. It is more than the average power penalty in Fig. 10. The reason is that the average power penalty can not be achieved for non-channel coded system. In other words, when channel coding is applied, then information embedded in the good symbols (with small phase/time synchronization error) can help the bad symbols (with large phase/time synchronization error) and the average power penalty can be approached. This is verified in next simulation.

We then compare the mutual information performance with different synchronization levels as in Fig. 12. Mutual information is more closely related to the channel coded performance than the uncoded BER. For perfect synchronization, we plot $I(s_1 \oplus s_2; r) = h(r) - h(r|s_1 \oplus s_2)$ at the relay node. For the non-perfect phase synchronization, we plot the mutual information when the phase offset is randomly distributed in $[-\pi/4, \pi/4]$ (this range corresponds to the case of no phase synchronization as mentioned in Sect. 3 and labeled as “No Phase Synchronization” in Fig. 12.) as

$$\frac{2}{\pi} \int_{-\pi/4}^{\pi/4} I(s_1 \oplus s_2; r|\theta) d\theta = \frac{4}{\pi} \sum_{k=0}^{19} I(s_1 \oplus s_2; r|\theta = 0.05k\pi/4). \tag{16}$$

For the non-perfect time synchronization error, we simply plot $I(s_1 \oplus s_2; r)$ with time offset randomly distributed in the given range. From Fig. 12, we can see that the SNR loss of no time synchronization is about 2.5 dB. This result is worse than the average SNR loss since the QPSK modulation limits the total mutual information of one symbol to 2 at most. The SNR loss of no carrier phase and carrier frequency synchronization is almost the same. It is much better than the theoretical upper bound in (9). The simulation results show that the PNC scheme is more robust to synchronization errors than the analysis as in Sect. 3.

6 Conclusion

This paper investigates the synchronization issues in Physical-layer Network Coding (PNC). We first study the penalty of synchronization errors in PNC. Both analysis and simulation show that PNC is robust to the synchronization errors. It has also been shown that the power penalty due to imperfect synchronization can be compensated by the larger SIR in the PNC transmission system. After that, we propose a new synchronization scheme in an N -node chain which performs PNC transmission. Last but not least, we have shown that global synchronization in PNC can be achieved without detrimental effects from synchronization-error propagation.

Acknowledgments This work is partially supported by NSFC (No. 60209016), NSF Guangdong (No. 10151806001000003) and NSF Shenzhen (JC201005250034A, JC201005250047A). It is also supported by the General Research Fund (No. 414911), and the AoE grant E-02/08, established under the University Grant Committee of the Hong Kong Special Administrative Region, China.

References

- Ojanpera, T., & Prasad, R. (1998). An over view of air interface multiple access for IMT 2000/UMTS. *IEEE Communications Magazine*, 36(9), 82–91.
- Pham, T., & Nguyen, H. (2010). Decorrelate-and-forward relaying scheme for multiuser wireless code division multiple access networks. *IET Communications*, 4, 443.
- Ng, P. C., & Liew, S. C. (2007). Throughput analysis of IEEE802.11 multi-hop ad-hoc networks. *IEEE/ACM Transactions on Networking*, 15(2), 309–322.
- Zhang, S., Liew, S., & Lam, P. (2006). Physical layer network coding. *ACM Mobicom2006*.
- Pun, M., Morelli, M., & Kuo, C. J. (2006). Maximum likelihood synchronization and channel estimation for OFDMA uplink transmissions. *IEEE Transactions on Communications*, 54(4), 726–736.
- Morelli, M. (2004). Timing and frequency synchronization for the uplink of an OFDMA system. *IEEE Transactions on Communications*, 52(2), 296–306.
- Elson, J., Girod, L., & Estrin, D. (2002). Fine-grained network time synchronization using reference broadcasts. In *Proceedings of OSDI*.
- Ganerwal, S., Kumar, R., & Srivastava, M. B. (2003). Timing-sync protocol for sensor networks. In *Proceedings of the 1st international conference on embedded networked sensor systems*, November 05–07, Los Angeles, California, USA.
- Tu, Y. -S., & Pottie, G. J. (2002). Coherent cooperative transmission from multiple adjacent antennas to a distant stationary antenna through AWGN channels. In *Proceedings of IEEE vehicular technology conference (VTC'02)* (pp. 130–134).
- Mudumbai, R., Wild, B., Madhow, U., & Ramch, K. (2006). Distributed beamforming using 1 bit feedback: From concept to realization. In *Proceedings of Allerton conference on on communication, control, and computing*.
- Mudumbai, R., Barriac, G., & Madhow, U. (2007). On the feasibility of distributed beamforming in wireless networks. *IEEE Transactions on Wireless Communication*, 6(5).
- Brown, D. R., III, & Poor, H. V. (2008). Time-slotted round-trip carrier synchronization for distributed beamforming. *IEEE Transactions on Signal Processing*, 56, 5630–5643.
- Brown, D. R., III, Prince, G., & McNeill, J. (2005). A method for carrier frequency and phase synchronization of two autonomous cooperative transmitters. In *Proceedings of 5th IEEE signal processing advances wireless communications*, New York, NY, June 5–8, pp. 278–282.
- Naqvi, H., Berber, S. M., & Salcic, Z. (2009). Performance analysis of collaborative communication in the presence of phase errors and AWGN in wireless sensor networks. In *Proceedings of the international conference on wireless communications and mobile computing: connecting the world wirelessly*.
- Wu, Y., Chou, P. A., & Kung, S. Y. (2004). Information exchange in wireless networks with network coding and physical layer broadcast. Technical Report MSR-TR-2004-78, Microsoft Research, Redmond WA, August 2004.
- Katti, S., Rahul, H., Hu, W., Katabi, D., Medard, M., & Crowcroft, J. (2008). XORs in the air: Practical wireless network coding. *IEEE/ACM Transactions on Networking*, 16(3).

17. Zhang, S., Liew, S., & Lu, L. (2008). Physical layer network coding schemes over finite and infinite fields. In *Proceedings of Globecom*, USA.
18. Koike-Akino, T., Popovski, P., & Tarokh, V. (2009). Optimized constellations for two-way relaying with physical layer network coding. In *IEEE Journal on Selected Area in Communications* (Vol. 27, pp. 773–787).
19. Zhang, S., & Liew, S. (2010). Applying physical layer network coding in wireless networks. *Eurasip Journal on wireless networks and communication*, 2010 (2010), 870268.
20. Jagannathan, S., Aghajan, H., & Goldsmith, A. (2004). The effect of time synchronization errors on the performance of cooperative MISO systems. In *Proceedings of IEEE Globecom* (pp. 102–107).
21. Zhang, S., & Liew, S.C. (2009). Channel coding and decoding in a relay system operated with physical-layer network coding. *IEEE Journal on Selected Areas in Communications*, 27(5), 788–796.
22. Zhang, S., Liew, S. C., & Lam, P. (2006). On the synchronization of physical layer network coding. In *Proceedings of IEEE information theory workshop*, China.
23. Proakis, J. G. (1995). *Digital communications*. New York: McGraw-Hill.
24. Nam, W., Chung, S., & Lee, Y. (2008). Capacity bounds for two-way relay channels. In *Proceedings of international Zurich seminar on communications (IZS 2008)*, Zurich, Switzerland.
25. Zhang, S., & Liew, S. C. (2010). Physical layer network coding with multiple antennas. In *Proceedings of IEEE WCNC2010*.
26. Lu, L., & Liew, S. C. (2011). Asynchronous physical layer network coding. Arxiv preprint arXiv:1105.3144, 2011-arxiv.org.
27. Wang, D., Fu, S., & Lu, K. (2009). Channel coding design to support asynchronous physical layer network coding. In *Proceedings of IEEE Globecom'09*. Honolulu, HI, November 30–December 4.
28. Lu, L., Wang, T., Liew, S. C., & Zhang, S. Implementation of physical layer network coding. Phycomm (submitted). Available at: <http://arxiv.org/abs/1105.3416>.
29. Fu, S., Lu, K., Zhang, T., Qian, Y., Chen, H.-H. (2010). Cooperative wireless networks based on physical layer network coding. *IEEE Wireless Communications*, 17(6), 86–95.
30. Liew, S., Zhang, S., & Lu, L. (2011). Physical-layer network coding: Tutorial, survey, and beyond. PhyComm (submitted). Online version: Arxiv preprint arXiv:1105.4261, 2011-arxiv.org.
31. Gupta, P., & Kumar, P. R. (2000). The capacity of wireless networks. *IEEE Transactions on Information Theory*, 46, 388–404.

Author Biographies



Shengli Zhang received his B.E. degree in electronic engineering and the M.E. degree in communication and information engineering from the University of Science and Technology of China (USTC), Hefei, China, in 2002 and 2005, respectively. He received the Ph.D. degree in the Department of Information Engineering, the Chinese University of Hong Kong (CUHK), in 2008. From 2002 to 2005, he was with the Personal Communication Network and Spread Spectrum (PCN & SS) Laboratory, USTC, as a Research Engineer involved in several National 863 Research Projects including the Beyond-3 Generation of Mobile System in China (FUTURE Plan). From 2002 to 2005, he was also a Research Engineer of the UTStarcom Wireless Soft Research Center, Hefei, China, involved in the research and implementation of the WCDMA communication systems. From Oct. 2008, he was a Research Associate in CUHK. Now, he is an assistant professor with the Communication Engineering Department, Shenzhen University, China. His current research interests include wireless networks, wireless communication, physical layer network coding, and cooperative wireless networks.



Soung-Chang Liew received his S.B., S.M., E.E., and Ph.D. degrees from the Massachusetts Institute of Technology. From 1984 to 1988, he was at the MIT Laboratory for Information and Decision Systems, where he investigated Fiber-Optic Communications Networks. From March 1988 to July 1993, he was at Bellcore (now Telcordia), New Jersey, where he engaged in Broadband Network Research. He has been Professor at the Department of Information Engineering, the Chinese University of Hong Kong, since 1993. He is Adjunct Professor at Peking University and Southeast University, China. Prof. Liew's current research interests include wireless networks, Internet protocols, multimedia communications, and packet switch design. Prof. Liew's research group won the best paper awards in IEEE MASS 2004 and IEEE WLN 2004. Separately, TCP Venó, a version of TCP to improve its performance over wireless networks proposed by Prof. Liew's research group, has been incorporated into a recent release of Linux OS. In addition, Prof. Liew initiated and built the first inter-

university ATM network testbed in Hong Kong in 1993. More recently, Prof. Liew's research group pioneers the concept of Physical-layer Network Coding (PNC). Besides academic activities, Prof. Liew is also active in the industry. He co-founded two technology start-ups in Internet Software and has been serving as consultant to many companies and industrial organizations. He is currently consultant for the Hong Kong Applied Science and Technology Research Institute (ASTRI), providing technical advice as well as helping to formulate R&D directions and strategies in the areas of Wireless Internetworking, Applications, and Services. Prof. Liew is the holder of eight U.S. patents and Fellow of IET and HKIE. He currently serves as Editor for IEEE Transactions on Wireless Communications and Ad Hoc and Sensor Wireless Networks. He is the recipient of the first Vice-Chancellor Exemplary Teaching Award at the Chinese University of Hong Kong. Publications of Prof. Liew can be found in www.ie.cuhk.edu.hk/soung.



Hui Wang received his B.S., M.S. and Ph.D. degrees from Xi'an Jiaotong University, in 1990, 1993, and 1996, respectively. He is now a professor in the College of Information Engineering, Shenzhen University. His research interests include wireless communication, signal processing, and distributed computing systems, in which, he is the author or co-author of more than 50 international leading journals, conferences and book chapters.